Plasma functionalization procedure for antibody immobilization for SU-8 based sensor

Immacolata Angelica Grimaldi[a],*, Genni Testa[a], Gianluca Persichetti[a], Fausta Loffredo[b], Fulvia Villani[b], Romeo Bernini[a]

[a]Institute for Electromagnetic Monitoring of the Environment (IREA), National Research Council (CNR), Naples, Italy

[b]Italian National Agency for New Technologies, Energy and Sustainable Economic Development (ENEA), Portici Research Center, P.le Enrico Fermi 1, 80055 Portici (Naples), Italy

[*]Corresponding author. Email address: grimaldi.a@irea.cnr.it; phone:+39 081 7620644

Abstract

In this paper, we report the study on a new protocol for the immobilization process of antigen/antibody assay on SU-8 layers by oxygen plasma treatment. Plasma treatments, at different plasma powers and for different duration times, are performed and their effects on immobilization efficiency are studied. The chemical properties and the surface morphology of SU-8 before and after the functionalization and immobilization of (IgG) are then verified by Raman spectroscopy and atomic force microscopy (AFM). An increase of the surface roughness of SU-8 layers is observed after the oxygen plasma treatment and an intensity variation of functional groups is also evidenced. To demonstrate the validity of the process the distribution of IgG immobilized on SU-8 surfaces is detected by fluorescence microscopy measurement after incubation with fluorescein isothiocyanate (FITC)-tagged anti-human IgG. An increase of the amount of the adsorbed protein of about 20% and a good repeatability on antigen/antibody distribution on the surface are detected for IgG on plasma treated substrates. Finally, label free measurements are performed by SU-8 optical ring resonators reaching detection limits of 0.86 ng cm^{-2}. The proposed approach offers a smart protocol for IgG immobilization on SU-8 substrate that can be easily extended to different antigen/antibody assay and polymeric materials for the realization of high performance immunosensors.

Keywords

Optical biosensor, Immunoglobulin G, Surface immobilization, Biosensing, Microring resonator

1. Introduction

Polymers are emerging materials in the development of biological micro-opto-electro-mechanical systems (bio-MOEMS) thanks to their physical and chemical properties. One of the most exploited polymeric material for optical and microelectromechanical sensors is SU-8. It is an epoxy based polymer with excellent optical, mechanical and thermal stability. The high polymerization efficiency under UV irradiation and the direct patternability in a single lithographic step make SU-8 attractive for communications, microfluidics and biosensing applications [Zhang et al., 2001; Grimaldi et al., 2014]. In the latter case, different structures are reported in literature for biosensing, such as microwells [Blagoi et al., 2008], microcantilever [Joshi et al.,2007a], planar waveguides [Jiang et al., 2008] and ring resonator [Salleh et al., 2013]. Among the optical sensors, polymeric microring resonators offer a lot of advantages such as easy of fabrication by lithographic or imprinting technology, reduced dimensions without losing in detection limit and output signal and their employment for mass production. Additionally, their working mechanism based on the use of the evanescent field as optical transduction principle allows the development of biosensors, where the antibody is usually immobilized on the sensor surface and the binding of the antigen can be controlled and followed in real-time [Washburn et al., 2009; Grimaldi et al., 2015]. The immobilization process of antibodies on an assay surface is a crucial step in the immunoanalysis, guaranteed by the high specificity of the antigen/antibody binding. Indeed, the specific recognition process and the high affinity of antigen/antibody interactions allow the

identification in complex sample matrices in competitive and noncompetitive assay, turning the sensing process into detectable physical or chemical signals [Densmore et al.,2009; Sai et al., 2010; Goh et al., 2005; Caruso et al., 1996; Jung et al., 2008; Tombelli et al., 2015].

Reliability, reproducibility, stability and binding activity of antibody immobilization onto sensing surface are key parameters that must to be taken into account in the immunosensor development and are influenced by the coupling chemistry [Qin et al.,2007; Kamisetty et al., 2006; Brynda et al., 1999; Vashist et al.,2006]. In particular, the molecular packing of the proteins at the liquid-surface interface is mainly based on two important mechanisms: adsorption and covalent immobilization. The covalent immobilization method requires chemical modification of the functional groups on the surface by using organofunctional silanes [Joshi et al., 2007a], pyrolytic dissociation of ammonia [Joshi et al., 2007b], chemical treatments [Deepu et al., 2009] and cerium ammonium nitrate (CAN) treatment [Blagoi et al., 2008]. All these wet surface modification methods usually use harsh chemicals and are long time consuming. On the other hand, the physical adsorption is the simplest immobilization method, based on strong electrostatic interactions between the proteins and the polymeric material, with remarkable advantages such as no chemical reagent consumption and no conformational change or disruption of proteins. The main drawbacks are related to repeatability and stability of the immobilization process. The employment of dry surface modification methods, such as oxygen plasma treatment, have been previously investigated in literature as promising techniques for optimizing and improving the adsorption efficiency on surface of polymers such as poly(methyl methacrylate) (PMMA) [Tsougeni et al., 2010], hexamethyldisiloxane [Yeo et al., 2006], polycarbonate and Zeonex [Rucker et al., 2005]. The oxygen plasma technique, compared to other techniques, is very cost-effective, environmental friendly and allows the modification of chemico-physical properties without altering the bulk properties. Moreover, other advantages of plasma method over other techniques include the minimization of thermal degradation, short treatment time and the selection of the desired functional groups [Selim et al., 2007]. The oxygen plasma treatment has demonstrated to increase the binding strength and the active site available for protein by increasing the surface roughness and the chemico-physical activation of functional groups on polymer surface [Yuan et al., 2009]. Moreover, different effects in terms of surface roughness, functional groups and, hence, protein adsorption efficiency can be induced by plasma treatment on different polymers, significantly modifying their chemico-physical selectivity. An accurate choice of substrate and optical active materials can significantly reduce the aspecific adsorption and, hence, the background noise. Last but not least, the transferability of the immobilization protocol from the laboratory to mass production scale is an additional aspect that should be taken into account for the development of an immunosensor. However, since the plasma treatments, acting as polymer etching, may damage the structural properties of sensing devices [Joshi et al., 2007b], an accurate study on plasma power and treatment effects on surface microstructure need to be performed.

In this work, we firstly explore the effects of the oxygen plasma on SU-8 surface on the immobilization efficiency of the IgG protein. We demonstrate the immunosensing capability of our device using human IgG as antibody and FITC tagged anti-human IgG as antigen. Studies on plasma powers and on treatment duration times are performed on SU-8 layers and the optimal conditions are evaluated by fluorescence analysis. Optical, chemical and morphological analyses of activated substrates before and after the immobilization process are performed by AFM and Raman spectroscopy. The immobilization efficiency, the repeatability of the binding mechanism and the surface uniformity are also evaluated by microscope fluorescence measurements, resulting in an optimization protocol that improves the device performances. Finally, the plasma effects on the sensing microstructures and the feasibility of the proposed approach are demonstrated by label free measurements using SU-8 based optical ring resonators.

2. Materials and methods

SU-8 films are realized on 2 mm-thick poly(methyl methacrylate) (PMMA) substrate. The PMMA sheets are cleaned with isopropyl alcohol and dried on hot plate at 70°C for 30 minutes. Negative SU-8 2002 (Microchem Corp.) is spin-coated at 3000 rpm onto PMMA substrate to obtain 2 μm thick layers. A pre-bake of 10 min at 70°C to evaporate the solvent is followed by UV curing process. After the UV exposure, the film is post-baked for polymer crosslinking. SU-8 microring resonators are realized on 2 mm-thick PMMA sheet by direct laser writing photolithographic process (Heidelberg GmbH, μPG 101) on 2μm thick layers with the same process steps of homogenous films. The ring resonator has a diameter of 280 μm, coupled to a straight bus waveguide 3 μm wide and 2 μm height to preserve the monomodal condition at 1550 nm [Grimaldi et al., 2015].

The microfluidic channel (500 μm width and 100 μm height) used to deliver the sample to the ring, is manufactured in PDMS by a standard replica molding process. When brought in contact with the PMMA substrate, a spontaneous adhesion is formed.

For biosensing experiments, bovine serum albumin (BSA), PBS ($1\times$ phosphate-buffered saline w/o Ca^{2+} and Mg^{2+}; pH 7.4), Tween 20, human IgG and anti-human IgG antibody labeled with fluorescein isothiocyanate (FITC) are purchased from Sigma Aldrich and used as received.

A microwave plasma generator (13.56 MHz, Diener Electronic) is used for plasma treatment.

The surface morphology of the SU-8 layers and the IgG immobilized on the surfaces are analyzed using an atomic force microscope (AFM, Veeco, Dimension Digital Instruments Nanoscope IV) in tapping mode configuration. The chemical properties are investigated by Raman spectroscopy (Renishaw InVia Reflex Raman spectrometer) using a 514.5-nm excitation source. Fluorescence images are acquired with inverted fluorescence microscopy (Motic AE31) equipped with high sensitivity CCD camera (Watec). All images are taken in the same ambient conditions at room temperature.

2.1 IgG immobilization protocol

Considering that the binding mechanism of IgG on SU-8 surface is physical adsorption, an accurate definition of immobilization protocol has to be defined in order to guarantee a good repeatability and stability of the overall process. Indeed, oxygen plasma treatment improves the binding strength and the sites available for IgG adsorption by modifying the chemico-physical selectivity and the surface roughness, with a consequent optimization of the molecular packing of the proteins. The experimental protocol followed for antibodies immobilization onto SU-8 surface is schematically represented in figure 1. An oxygen flow of 500 sccm at a pressure of approximately 5×10^{-4} bar is maintained with a plasma power of 25W (P_1) and 50W (P_2) for different treatment durations (from 0 to 30 min), as showed in figure 1a. The carboxylic groups can be used to bind biologically IgG. For SU-8 films, the immobilization of IgG (concentration of 100 μg/mL in PBS) is performed by a pre-incubation step of 15min at 37°C followed by a manual deposition of 3μL droplets and incubation for 1h at room temperature on PBS washed substrates. Loosely adsorbed antibodies and the non-specific adsorption sites on the activated surface are blocked with a buffer called PBST-BSA, consisted of 1 mg/mL bovine serum albumin (BSA) and 0.05% (v/v) Tween20 diluted in PBS (fig.1c). The SU-8 films are rinsed three times in PBST-BSA and gently dried with air flow. The binding of FITC tagged anti-human IgG at different concentration (0.033, 0.066, 0.33, 1, 3.3 and 33 μg/mL) is accomplished by immersing the SU-8 films for 1h at room temperature (fig. 1d), rinsed three times with PBS and observed by inverted fluorescence microscopy.
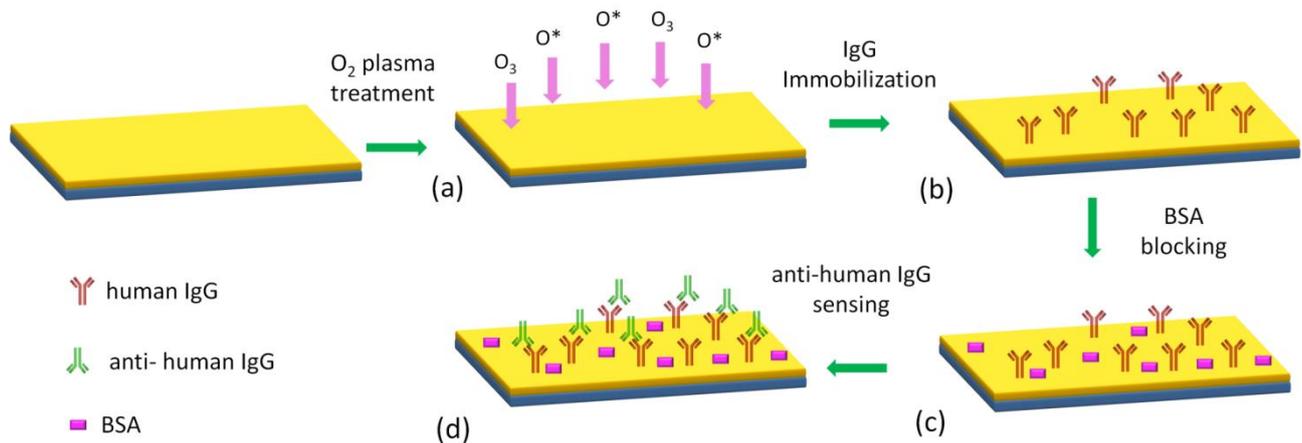
Fig. 1 Schematic representation of immobilization process of IgG on SU-8 substrate and of anti-human IgG binding: a) oxygen plasma treatment for nanotexturing and surface chemical modification of SU-8, b) IgG immobilization on surface, c)blocking with a BSA based solution, d) incubation of anti-human IgG to evaluate the bioactivity of the immobilized IgG.

3. Results and discussion

The effects of the plasma treatments on the immobilization process of IgG are studied by fluorescence microscopy. Two different powers (P_1= 25W and P_2=50W) are employed on 2 μm thick spin-coated SU-8 films. As reference, the same experiments are performed onto PMMA substrate, treated with oxygen plasma at the same powers and duration times used for SU-8. The analyses of the fluorescence intensity of the labeled anti-human IgG (100 µg/mL concentration) immobilized on activated SU-8 and PMMA substrate as function of oxygen plasma treatment time (0, 1, 5, 10, 20, and 30 min) for both P_1 and P_2 are reported in figure 2 a) and b), respectively. From figure 2 it can be noticed that the fluorescence signal of untreated SU-8 (zero time) is lower than plasma treated substrate, which clearly indicates an increase of the amount of immobilized antigen/antibody induced by plasma exposure. For SU-8 substrate, by increasing the oxygen plasma treatment time the fluorescence intensity starts to build up following an exponential behavior. This can be attributed to an increase of IgG proteins adsorbed onto SU-8 due to the surface nanotexturing and chemical functionalization generated by plasma treatment. Indeed, it has been previously demonstrated that the oxygen plasma process onto SU-8 resist offers the most effective and stable hydrophilization process and causes an increase of the root mean square (rms) surface roughness [Ashraf et al., 2015]. An enhancement of about 20% of the fluorescence intensity and, hence, of the immobilization efficiency with respect to the untreated surface can be appreciated after only 5min. Using one-way analysis of variance (ANOVA), the fluorescence intensities after 5 min of plasma treatment are significantly different with respect to the untreated surfaces for both plasma conditions: *p-value*=0.011 at 25W and *p-value*=0.024 at 50W. These values, lower than 0.05, indicate that the oxygen plasma can be considered as a suitable method to improve the performance of the immobilization protocol of IgG on SU-8 surface comparable with those reported by Deepu et al., 2009, using glycine or mercapto undecanoic acid as crosslinker molecules. As it is shown in figure 2, longer treatment does not further increase the fluorescence intensity, i.e. protein immobilization, which saturates after 5 min for both P_1 and P_2. The plateau of the fluorescence intensity curve for treatments longer than 5 min indicates a saturation effect on the protein adsorption. This could be due by the plasma induced surface porosity that, over certain level, can hinder the immobilization process [Tsougeni et al., 2010]. As comparison, plasma exposures on PMMA substrate shows negligible effects on the IgG immobilization with no evidence of fluorescence intensity variations (One-way ANOVA, *p-value* =0.28 at 25W and *p-value* =0.66 at 50W). Moreover, it is important to highlight that PMMA shows significantly

lower fluorescence intensity compared to bare SU-8 and also under both plasma treatment conditions, indicating worse immobilization efficiency. We demonstrate that the oxygen plasma modify the immobilization efficiency on different polymers and, hence, their chemico-physical selectivity. Under these conditions PMMA, used as substrate, and SU-8, employed as optical active materials, can optimize the sensing performance of immunosensors.
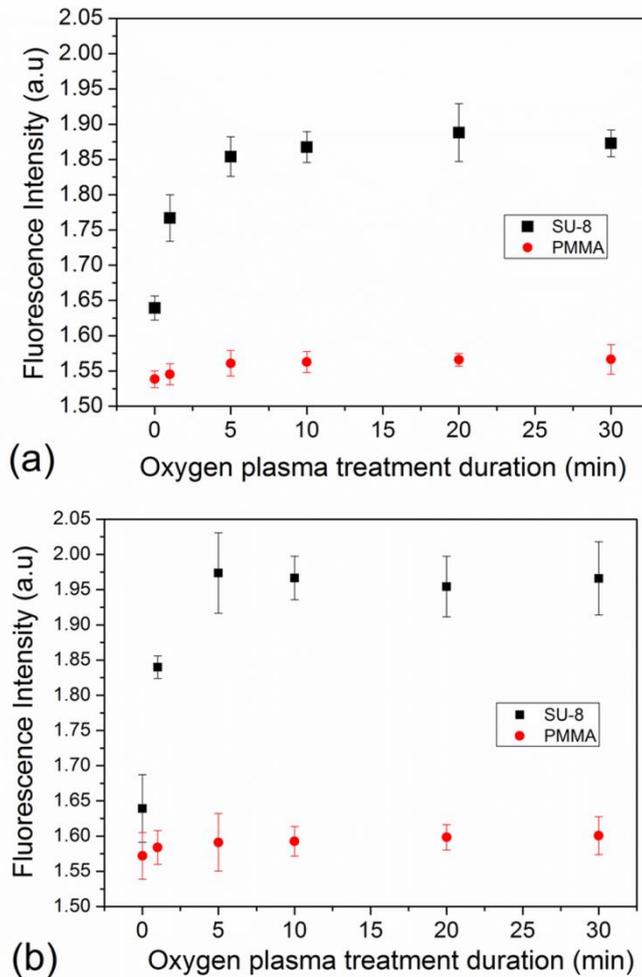

Fig. 2 Fluorescence intensity values as function of oxygen plasma exposure time for SU-8 (black square) and PMMA (red circle) substrates coated with IgG and incubated for 1h with anti-human IgG: a) 25W and b) 50W plasma power.

In order to investigate the differences in the fluorescence measurements, we study the water contact angle for untreated and plasma treated SU-8 films immediately after the plasma treatment and after 7 days of storage. The analysis of the results, reported in figure S1, indicates an increase of the wettability after only 15 sec of plasma treatment. Indeed, the contact angle reduces from $89°\pm5°$ to $25°\pm4°$ and to $15°\pm3°$ for 25W and 50W, respectively. When the treatment duration is equal to 60 sec, an almost full wetting takes place with a contact angle of only $7°\pm2°$ regardless of the applied plasma power. The further treatments extension increases the wetting, thus leading to smaller contact angle measurements. Moreover, the long term effects of plasma treatment are explored by measuring the contact angle on O_2-plasma treated SU-8 layers (treatment duration 600 sec) after 7 days storage in ambient condition. At fixed treatment duration the contact angle of aged films increases to $46°\pm3°$ and to $15°\pm3°$ for 25W and 50W, respectively. These differences in the aging

effects can be explained by considering that the low power treatment has less effect on the surface topography and on the long term surface chemistry, inducing a different aging effect.

The chemical properties of SU-8 films before and after oxygen plasma treatment are examined by Raman spectroscopy. The Raman spectra of bare and plasma treated SU-8 (5 min) at 25W and 50W are reported in table S1 and showed in figure 3a: the arrows mark typical peaks of interest and the logarithmic ordinate axis shows a better view of small changes. Usually the polymerization of SU-8 resist proceeds via generation of Lewis acid which is detached from the monomer molecules and promotes cationic cross-linking under UV exposure. The curing process leads to the reduction of bands at 895 cm^{-1}, associated to acetic acid, and the 738-762 cm^{-1}, associated to C-S bond, almost absent in our measurements, symptom of a complete curing of the investigated substrates [Suzuki et al., 2012]. The peak centered at 1452 cm^{-1} can be associated to CH_2 and CH_3 groups: the presence of methyl group (-CH_3) may be cause of hydrophobicity of the resist surface, whose contact angle is near to 90° [Kumar and Sharma, 2015]. A small decrease of the peaks associated to CH_3, CH_2 and C-C groups can be appreciated after O_2 plasma action, as expected from contact angle measurements.

In order to verify the functionalization with IgG protein of SU-8 substrate, Raman measurements are performed on both 25W and 50W plasma treated substrates. The treated substrates are spotted with 50 µL IgG protein at 100 µg/mL concentration and, after 1h for the immobilization process, are washed three times with PBST-BSA solution. Raman spectra of IgG immobilized on SU-8 treated with plasma power of 25W and 50W are reported in figure 3b. As shown in figure 3b, a new peak at 1638 cm^{-1} appears in the Raman spectra after functionalization, typical of Amide I chemical structure of IgG. Moreover, the Amide III band of IgG at 1240 cm^{-1} has a relative weak peak, undistinguishable in the Raman spectra due to strong intensity of the 1220-1260 cm^{-1} band related to SU-8 resist. Moreover, the intensity of the peak at 1638 cm^{-1} increases at higher plasma power, as yet observed from fluorescence analyses reported in figure 2. All these characterizations confirm the successful of the immobilization protocol employed for SU-8 resist.
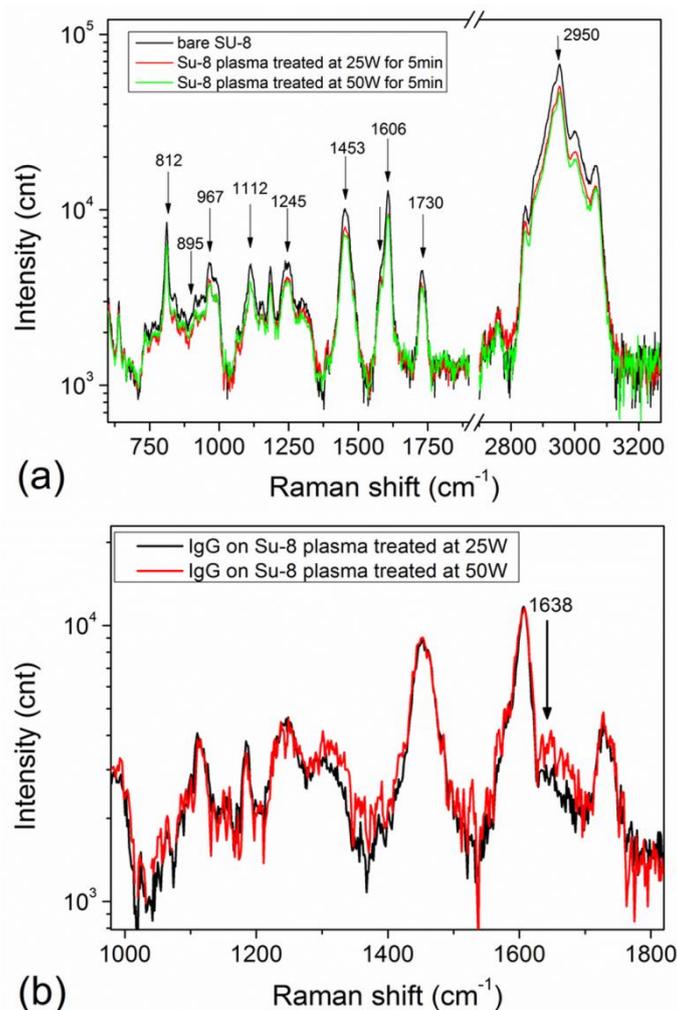
Fig. 3 (a) Raman spectra of untreated SU-8 (black line), oxygen plasma treated at 25W for 5 min (red line) and at 50W for 5min (green line); (b) raman spectra after functionalization with IgG of SU-8 layers plasma treated at a) 25W for 5min and b) 50W for 5min.

The main morphological features of the untreated and plasma treated films are evidenced in 2D and 3D AFM images, reported in figure 4. The rms roughness of the unmodified SU-8 surface is 0.213 nm (fig 4a,e). The surface roughness of plasma treated SU-8 films is slightly modified after plasma treatment and it is found to be almost independent on the plasma power: the rms roughness is 1.628 nm and 1.599 nm for P_1 and P_2, respectively. As anticipated, the oxygen plasma treatment modifies the surface morphology inducing a visible grain-structure (i.e. surface porosity) with respect to the untreated one. For the plasma action at 25 W, the average size of the grains is in the range of 15-25 nm (fig. 4b, f). By increasing the applied plasma power up to 50 W, the average size of the surface grains increases, as expected, and ranges among 23-29 nm (fig. 4c, g). The immobilization of the IgG onto the activated substrates (fig. 4d,h) covers the granular structure of the plasma O_2-treated SU-8 surface and induces an increase of the surface roughness of 2.242 nm.
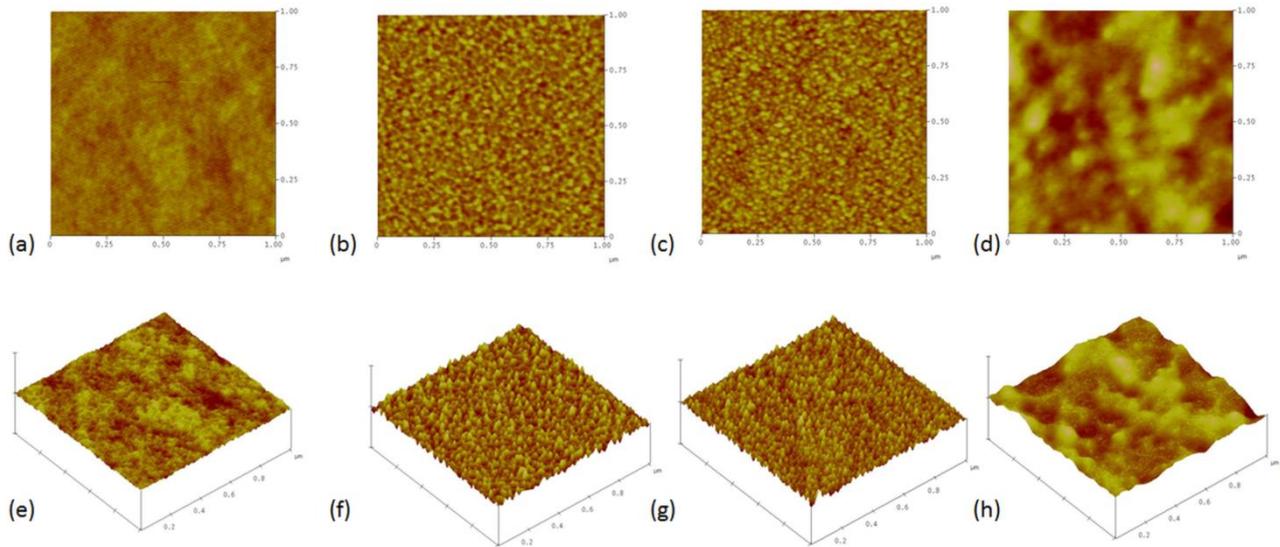
Fig. 4 2D (up) and 3D (bottom) topographic AFM images of SU-8 a,e)untreated reference; b,f)plasma treated at 25W for 5min; c,g) plasma treated at 50W for 5min; d,h) after IgG immobilization.

4. Immunosensing analysis

Following the developed experimental protocol, the fluorescence intensity of labeled anti-human IgG immobilized onto IgG functionalized SU-8 layer as function of the concentration (0.033, 0.066, 0.33, 1, 3.3 and 33 μg/mL) is reported in figure 5. The fluorescence intensity follows a sigmoidal behaviour, as expected, with a saturation condition for anti-human IgG concentration higher than 3.3 μg/mL. The surface homogeneity of the immobilization procedure has been evaluated on ten different samples. Variations in the range of 2-5% in the fluorescence signal are detected, a clear indication of the good reliability of the developed immobilization process.
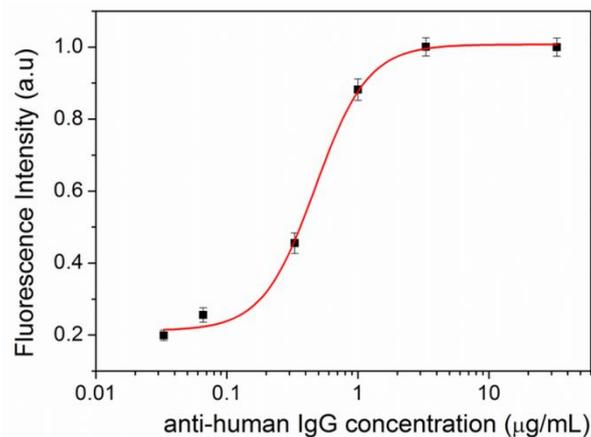

Fig. 5 Fluorescence intensity from plasma treated SU-8 ring resonator as function of anti-human IgG concentration.

Using the optimized condition for immunoassay on SU-8, we realize a sensing platform structure based on microring resonator, evanescently coupled with a bus waveguide. In order to study the effects of the plasma treatment duration on the structural and optical properties of the SU-8 ring resonators, the quality (Q) factor [Grimaldi et al., 2015], that characterize the sensing performance, has been monitored. In figure 6a the Q-factor variations with respect to untreated one are reported as function of the plasma duration for 25W and 50W plasma power, respectively. The analysis of the results for 25W power plasma indicates an improvement of the quality factor of 1.1 for 5 min plasma and a decrease for longer plasma treatment. The

first effect can be associated to an increase of C=O and COO groups caused by oxidation with reactive species generated in the atmospheric oxygen, chemically substituting to C-H bonds on the SU-8 surface after the treatment [Walther et al., 2010; Airoudj et al., 2008]. The absorption of the C-H bonds occurs in the near-infrared region, the same range of the optical experiment, due to the coupling of the harmonics to the stretching vibration [Airoudj et al., 2008]. As the plasma treatment duration increases, the decreasing of the Q-factor can be associated to the scattering losses induced by structural modifications. Plasma treatment carried out with a power of 50W shows a monotonic decrease of the Q-factor up to 15% for 30min plasma action, without the presence of the peak observed at 25W for short treatment duration. For plasma power of 50W, the effects related to the introduction of C=O and COO functional groups are masked by the increasing of the scattering losses caused by the increased roughness. Indeed, during the plasma treatments the oxygen atoms cause an etching effect on SU-8 that affect the structural properties, as demonstrated by AFM analysis (fig. 4c,g). These results, together with the fluorescence measurements, suggest that the best compromise between the immobilization efficiency and the optical performances is given by 5 min plasma treatment at power of 25W.
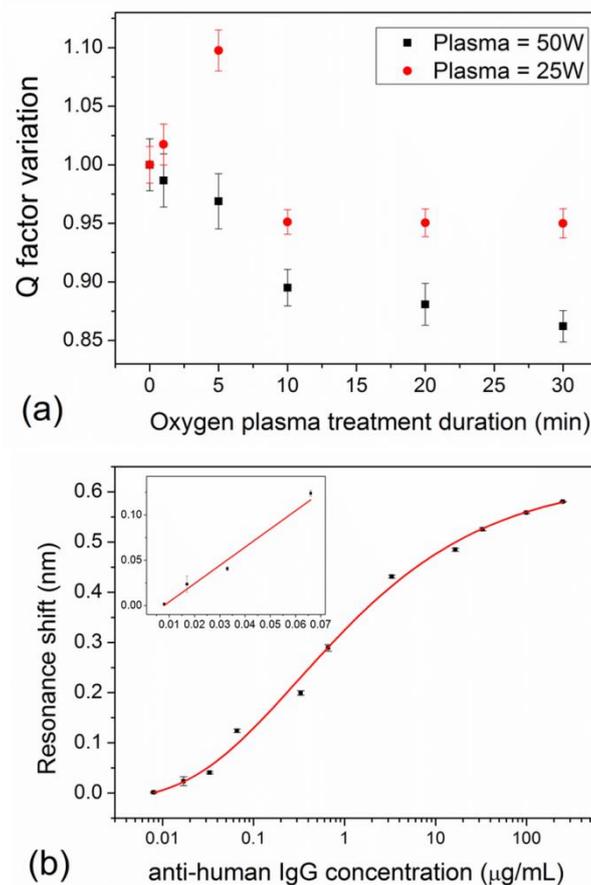

Fig. 6 (a) Q-factor of microring resonators after exposure to 25W (red circle) and 50W (black square) oxygen plasma as function of treatment duration. (b) Calibration curve of resonance shift as function of anti-human IgG concentration in log scale. The experimental points are fitted with a sigmoidal curve (red solid line). The inset shows the linear behaviour of the first four points in a linear concentration scale.

In order to evaluate the biosensing capability of immobilized IgG on plasma treated SU-8 based resonators, we perform quantitative measurements of anti-human IgG by evaluating the red shift effect of the resonance peak in the transmitted signal. The surface sensitivity is estimated by using different concentrations of anti-human IgG (from 0.008 µg/mL to 250 µg/mL), covalently bounded to human IgG on activated SU-8

microring resonator at 25W for 5min. The flow rate of anti-human IgG is kept constant to 5µL/min and each solution is flowed for 20 min over the resonator surface. The calibration curve, obtained by evaluating the resonance shift as a function of the anti-human IgG concentration, is reported in figure 6b. The experimental points are well fitted with a sigmoidal curve, a clear indication of binding site limited reactions. The sensor response shows a linear behaviour up to 0.066 µg/mL (as reported in the inset of fig 6b), and a saturation condition at higher concentrations due to the total surface coverage with anti-human IgG. The sensitivity for surface mass detection is given by $S_m = \Delta\lambda/\sigma_p$, where $\Delta\lambda$ is the shift resonance at saturation and σ_p is the surface density of a molecular monolayer. The estimated value from figure 6b is $\Delta\lambda = 599$ pm, while the surface density of a compact anti-human IgG layer is $\sigma_p = 156$ ng cm^{-2} [Bonroy et al., 2006], giving a calculated sensitivity of $S_m = 3.83$ pm ng^{-1} cm^2. The surface mass detection limit is defined as the ratio between the sensor resolution R and the mass sensitivity S_m, previously determined:

$$L_m = \frac{R}{S_m}$$

For the sensor resolution R we follow the convention of using three times the standard deviation (3σ) of the baseline noise. From the experimental measurements, we estimate R=3.3 pm, giving a detection limits of L= 0.86 ng cm^{-2}.

Conclusion

In this work, we report the study on the immobilization protocol of IgG for the realization of an immunosensor based on SU-8 optical material. In particular, we showed that the oxygen plasma treatment is able to improve the immobilization efficiency of the protein on a SU-8 surface in a novel, robust and simple way. The immobilization process of human IgG on SU-8 polymer is evaluated for different plasma treatment durations and plasma powers. A high uniform distribution of protein coverage, proved by 2-5% variations of the fluorescence signal, and an increase of about 20% of the protein-binding capability are attributable to the surface nanotexturing effect and to the activation of functional groups due to oxygen plasma treatment, as shown by morphological and chemical analyses. The biochemical sensing by fluorescence analysis shows a sigmoidal behaviour with a saturation condition for antigen concentration higher than 3.3 µg/mL and a saturation condition at higher concentrations. The feasibility study of this protocol on microring resonators shows good sensing performances of the device with a calculated limit of detection of L= 0.86 ng cm^{-2}. Future work will be devoted to test the realized sensors in practical applications such as real blood serum sample. Indeed, the proposed approach, combining an efficient immobilization protocol with a real time sensing, can be scaled up for industrial applications for high performances sensitive immunoassay development.

Acknowledgements

References

Airoudj, A., Debarnot, D., Beche, B., Boulard, B., Poncin-Epaillard, F., 2008. Plasma Process. Polym. 5, 275–288.

Ashraf, S., Mattsson, C. G., Fondell, M., Lindblad, A., Thungström, G., 2015. Mater. Res. Express, 2 086501.

Blagoi, G., Keller, S., Johansson, A., Boisen, A., Dufva, M.,2008. Appl. Surf. Sci. 255, 2896–2902.

Bonroy, K., Frederix, F., Reekmans, G., Dewolf, E., De Palma, R., Borghs, G., Declerck, P., Goddeeris, B., 2006. J. Immunol. Methods 312, 167–181.

Brynda, E., Houska, M., Brandenburg, A., Wikerstal, A., Skvor, J., 1999, Biosens. Bioelectron. 14, 363–368.

Caruso, F., Rodda, E., Furlong, D. N., 1996. J. colloid interface sci. 178, 104–115.

Deepu, A., Sai, V.V.R., Mukherji, S. 2009. J. Mater. Sci.: Mater. Med. 20, S25-S34.

Densmore, A., Vachon, M., Xu, D.-X., Janz, S., Ma, R. , Li, Y.-H., Lopinski, G., Delâge, A., Lapointe, J., Luebbert, C. C., Liu, Q. Y., Cheben, P., Schmid, J. H., 2009. Opt. Lett. 34, 3598-3600.

Goh, J. B., Loo, R. W., Goh, M. C., 2005. Sens. Act. B 106, 243–248.

Grimaldi, I.A., Berneschi, S., Testa, G., Baldini, F., Nunzi Conti, G., Bernini, R., 2014. Appl. Phys. Lett. 105, 231114-1–231114-4.

Grimaldi, I. A., Testa G., Bernini, R., 2015. RSC Adv. 5, 70156–70162.

Jiang, L., Gerhardt, K. P., Myer, B., Zohar, Y., Pau, S., 2008. J. Microelectromech. Syst. 17, 1495-1500.

Joshi, M., Pinto, R., Rao, V. R., Mukherji, S., 2007a. Appl. Surf. Sci., 253, 3127–3132.

Joshi, M., Kale, N., Lal, R., Rao V. R., Mukherji, S., 2007b. Biosens. Bioelectron. 22, 2429–2435.

Jung, Y., Kang, H. J., Lee, J. M., Jung, S. O., Yun, W. S., Chung, S. J., Chung, B. H., 2008. Anal. Biochem. 374, 99–105.

Kamisetty, N. K., Pack, S. P., Nonogawa, M., Devarayapalli, K. C., Kodaki, T., Makino, K., 2006. Anal. Bioanal. Chem. 386, 1649–1655.

Kumar, V., Sharma, N. N., 2015. J. Appl. Polym. Sci. 132, 41934.

Qin, M., Hou, S., Wang, L., Feng, X., Wang, R., Yang, Y., Wang, C., Yu, L., Shao, B., Qiao, M., 2007. Colloids Surf. B: Biointerfaces 60, 243–249.

Rucker, V. C., Havenstrite, K. L., Simmons, B. A., Sickafoose, S. M., Herr, A. E., Shediac, R., 2005. Langmuir 21, 7621-7625.

Sai, V.V.R., Kundu, T., Deshmukh, C., Titus, S., Kumar, P., Mukherji, S., 2010. Sens. Act. B 143, 724–730.

Salleh, M. M., Glidle, A., Sorel, M., Reboud, J., Cooper, J. M., 2013. Chem. Commun. 49, 3095-3097.

Selim, K. M. K., Xing, Z.-C., Bae, H.-S., Kang, I.-K., 2007. Biomaterials Research 11, 139-150.

Suzuki, T., Morikawa, J., Hashimoto, T., Buividas, R., 2012. Proc. of SPIE 8249, 82490K–82490K-9.

Tombelli, S., Trono, C., Adinolfi, B., Chiavaioli, F., Giannetti, A., Eugen-Olsen, J., Bernini, R., Grimaldi, I. A., Persichetti, G., Testa, G., Baldini, F., 2015. Proc. of SPIE 9313, 93130W-1 – 93130W-6.

Tsougeni, K., Tserepi, A., Constantoudis, V., Gogolides, E.,2010. Langmuir, 26, 13883–13891.

Vashist, S. K., Raiteri, R., Tewari, R., Bajpai, R. P., Bharadwaj, L. M., 2006. J. Phys.: Conf. Series 34, 806–811.

Walther, F., Drobek, T., Gigler, A. M., Hennemeyer, M., Kaiser, M., Herberg, H., Shimitsu, T., Morfill, G. E., Stark, R. W., 2010. Surf. Interface Anal. 42, 1735–1744.

Washburn, A. L., Gunn, L. C., Bailey, R. C., 2009. Anal. Chem. 81, 9499–9506.

Yeo, S. H., Choi, C. R., Jung, D., 2006. J. Korean Phys. Soc., 48, 1325-1328.

Yuan, Y., He, H., Lee, L.J., 2009. Biotechnol. Bioeng. 102, 891-901.

Zhang, J., Tan, K. L., Hong, G. D., Yang L. J., Gong, H. Q., 2001. J. Micromech. Microeng. 11, 20–26.